Transactions of the Materials Research Society of Japan 31[2] 483-486 (2006)

Energy Source Properties of Tube Cathode Arc

S. Tashiro, M. Tanaka, M. Nakatani*, K. Tani* and M. Furubayashi*
Joining and Welding Research Institute, Osaka University, 11-1 Mihogaoka, Ibaraki, Osaka 576-0047
e-mail: tashiro@jwri.osaka-u.ac.jp
* Hitachi Zosen Corporation, 2-11, Funamachi 2-chome, Taisho-ku, Osaka 551-0022

Gas Tungsten Arc (GTA) is the most widely employed type of the plasma torch and enables to produce arc plasma with high energy density. Therefore it is suitable as a heat source especially for processes to require concentrating the heat input at a point but less effective for processes to require heating the target material uniformly. On the other hand, Tube Cathode Arc (TCA) to be a kind of GTA produces the arc plasma by introducing the shielding gas from the tip of the cathode. It has been studied as a heat source especially in low pressure, for example, for space welding or plasma CVD. As an application at the atmospheric pressure, it can be utilized for processes such as thermal spraying. In this paper, the basic heat source properties of argon TCA at the atmospheric pressure are numerically analyzed. Furthermore, the properties are compared with those for the conventional GTA.
Key words: Numerical analysis, Tube cathode, Heat input, Arc plasma, Argon

1. INTRODUCTION

Since a plasma torch can stabilize high temperature arc plasma by employing a shielding gas, it is used as a heat source. Gas Tungsten Arc (GTA) is the most widely employed type of the plasma torch and produces the arc plasma between a tungsten cathode and an anode material. It has high heating efficiency and highly controllable characteristics, and requires low cost for equipment investment. Furthermore, the target material can be heated without any chemical reaction by using an inert gas as the shielding gas. Therefore, it is widely utilized, for example, for material processing such as melting, cutting and welding [1], or decomposition, volume reduction and detoxification of toxic waste [2] and so on.

The heat source properties of GTA strongly depend on physical properties of the shielding gas. For instance, helium gas with low electrical conductivity or carbon dioxide with high specific heat causes the constriction of the arc plasma and, hence, enables to produce the arc plasma with high energy density [3]. Therefore, GTA is suitable especially for processes to require concentrating the heat input at a point but less effective for processes to require heating the target material uniformly.

On the other hand, Hollow Cathode Arc (HCA) to be a kind of GTA produces the arc plasma by introducing the shielding gas through the central hole of the hollow cathode. It has been studied as the heat source especially in lower pressure, for example, for space welding [4] or plasma CVD [5], because it is suitable to supply the shielding gas in the electrode gap. As an application at the atmospheric pressure, it can be utilized for thermal spraying [6]. In this case, since the target material such as powder is injected through the hollow cathode into the high temperature arc plasma near the cathode directly, it can be heated more efficiently. However, the heat source properties of HCA at the atmospheric pressure are not fully understood.

In this paper, HCA at the atmospheric pressure is termed as Tube Cathode Arc (TCA), because the mechanism of electron emission is different from that in low pressure. As the basic heat source properties of argon (Ar) TCA, the properties of the arc plasma and the heat input intensity into a water-cooled copper anode for various shielding gas flow rates are numerically analyzed. Furthermore, the properties are compared with those for the conventional GTA.

2. SIMULATION MODEL

The tungsten cathode, the arc plasma and the water-cooled copper anode are described in a frame of cylindrical coordinate with axial symmetry around the arc axis. The calculation domain is shown in Figure 1. The details of the cathodes for GTA and TCA are shown in Figure 2 (a) and (b), respectively. The outer diameter and the inner diameter only for TCA are 3.2mm and 1.6mm, correspondingly. The electrode gap is set to be 5mm. The arc current is set to be 150A. Ar is introduced at the flow rate of 10L/min. from the outside of the cathode on the upper boundary. Only for TCA, that at the flow rate of 0.1, 0.5, 1.0 or 2.0L/min. is additionally introduced through the hole of the tube cathode, which is defined as an inner shielding gas. The flow is assumed to be laminar, and the arc plasma is assumed to be under the local thermodynamic equilibrium (LTE). Azimuthally uniform expansion of the cathode spot is also assumed. The other numerical modeling methods are given in detail in our previous papers [7, 8]. The differential equations (1)-(6) are solved iteratively by the SIMPLEC numerical procedure [9]:

Mass continuity equation;

$$\frac{1}{r}\frac{\partial}{\partial r}(r\rho v_r)+\frac{\partial}{\partial z}(\rho v_z)=0 \qquad (1)$$

Radial momentum conservation equation;

$$\frac{1}{r}\frac{\partial}{\partial r}(r\rho v_r^2)+\frac{\partial}{\partial z}(\rho v_r v_z)=-\frac{\partial P}{\partial r}-j_z B_\theta+\frac{1}{r}\frac{\partial}{\partial r}\left(2r\eta\frac{\partial v_r}{\partial r}\right)+\frac{\partial}{\partial z}\left(\eta\frac{\partial v_r}{\partial z}+\eta\frac{\partial v_z}{\partial r}\right)-2\eta\frac{v_r}{r^2} \qquad (2)$$

Axial momentum conservation equation;

$$\frac{1}{r}\frac{\partial}{\partial r}(r\rho v_r v_z)+\frac{\partial}{\partial z}(\rho v_z^2)=-\frac{\partial P}{\partial z}+j_r B_\theta+\frac{\partial}{\partial z}\left(2\eta\frac{\partial v_z}{\partial z}\right)+\frac{1}{r}\frac{\partial}{\partial r}\left(r\eta\frac{\partial v_r}{\partial z}+r\eta\frac{\partial v_z}{\partial r}\right) \quad (3)$$

Energy conservation equation;

$$\frac{1}{r}\frac{\partial}{\partial r}(r\rho v_r h)+\frac{\partial}{\partial z}(\rho v_z h)=\frac{1}{r}\frac{\partial}{\partial r}\left(\frac{r\kappa}{c_p}\frac{\partial h}{\partial r}\right)+\frac{\partial}{\partial z}\left(\frac{\kappa}{c_p}\frac{\partial h}{\partial z}\right)+j_r E_r+j_z E_z-R \quad (4)$$

Current continuity equation;

$$\frac{1}{r}\frac{\partial}{\partial r}(rj_r)+\frac{\partial}{\partial z}(j_z)=0 \quad (5)$$

Ohm's law;

$$j_r=-\sigma E_r, j_z=-\sigma E_z \quad (6)$$

where t is time, h is enthalpy, P is pressure, v_z and v_r are the axial and radial velocities, j_z and j_r are the axial and radial component of the current density, g is the acceleration due to gravity, κ is the thermal conductivity, C_p is the specific heat, ρ is the density, η is the viscosity, σ is the electrical conductivity, R is the radiation emission coefficient, E_r and E_z are, respectively, the radial and axial components of the electric field defined by $E_r=-\partial V/\partial r$ and $E_z=-\partial V/\partial z$, where V is electric potential. The azimuthal magnetic field B_θ induced by the arc current is evaluated by maxwell's equation.

$$\frac{1}{r}\frac{\partial}{\partial r}(rB_\theta)=\mu_0 j_z \quad (7)$$

where μ_0 is the permeability of free space.

In the solution of Eqs. (1)-(6), special account needs to be taken at the electrode surface for effects of energy that only occur at the surface. At the cathode surface, additional energy flux terms need to be included in Eq. (4) for thermionic cooling due to the emission of electrons, ion heating, and radiation cooling. The additional energy flux for the cathode H_k is:

$$H_K=-\varepsilon\alpha T^4-|j_e|\phi_K+|j_i|V_i \quad (8)$$

where ε is the surface emissivity, α is the Stefan-Boltzmann constant, ϕ_K is the work function of the tungsten cathode, Vi is the ionization potential of argon, j_e is the electron current density, and j_i is the ion current density. At the cathode surface, for thermionic emission of electrons, j_e cannot exceed the Richardson current density J_R [10] given by:

$$|j_R|=AT^2\exp\left(-\frac{e\phi_e}{k_B T}\right) \quad (9)$$

where A is the thermionic emission constant for the cathode surface, ϕ_e is the effective work function for thermionic emission of the electrode surface at the local surface temperature, and k_B is the Boltzmann's constant. The ion-current density j_i is then assumed to be $|j|-|j_R|$ if $|j|$ is greater than $|j_R|$; where $|j|=|j_e|+|j_i|$ is the total current density at the cathode surface obtained from Eq. (5)

Similarly, for the anode surface, Eq. (4) needs additional energy flux terms for thermionic heating and radiation cooling. the additional energy flux for the anode H_A is:

$$H_A=-\varepsilon\alpha T^4+|j|\phi_A \quad (10)$$

where ϕA is the work function of the anode and | j | is the current density at the anode surface obtained from Eq. (5). The term including ϕA accounts for the heating of the anode by electrons, which delivers energy equal to the work function on being absorbed at the anode. The term is analogous to the cooling effect that occurs at the cathode when electrons are emitted.

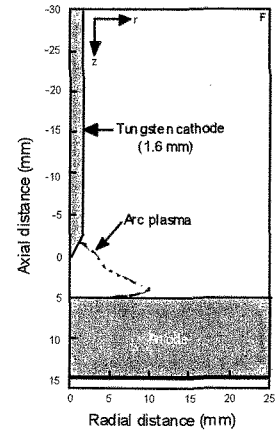

Fig. 1. Schematic illustration of simulation domain.

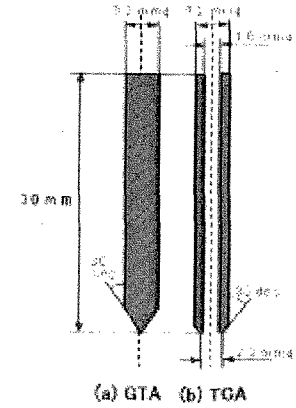

Fig. 2. Schematic illustrations of tungsten cathodes for GTA and TCA.

3. RESULTS AND DISCCUSION

Figure 3 shows two-dimensional distribution of temperature and fluid flow velocity for GTA. Figure 4-7 show those for TCA at the inner shielding gas flow rate of 0.1, 0.5, 1.0 and 2.0L/min., respectively. Figure 8-10 show radial distributions of heat input intensity, current density and surface temperate on the anode surface.

In the case of GTA, the current density near the arc axis becomes higher, since the arc current channel on the cathode tip is constricted at a point. The enhanced electromagnetic pinch force accelerates the cathode jet velocity up to 217m/s and, thus, leads to the high arc pressure to the anode surface. The increase in Joule heating due to the high current density lifts the plasma temperature near the cathode up to 17000K. It is obvious that the plasma temperature distribution becomes less uniform due to the steep temperature gradient near the cathode. On the other hand, the heat input onto the anode surface is concentrated near the arc axis especially due to the concentration of the thermionic heating which is proportional to the current density. Consequently, the heat input intensity and max. anode surface temperature reach 5000W/cm^2 and 610K, respectively.

Now, turn to the results for TCA. The current density lowers especially near the cathode due to the expansion of the arc current channel caused by the large area of the cathode tip. It leads to the cathode jet velocity of approximately 50m/s which is 25% of the GTA and, thus, the lower arc pressure. In contrast to the GTA, a remarkable peak doesn't appear in the plasma temperature distribution, since the max. plasma temperature reaches only 11000K which is 60% of the GTA. It is found that although the plasma near the arc axis tends to be cooled by the shielding gas, a large volume of the uniform high temperature plasma can be produced for the lower inner shielding gas flow rate. The max. heat input intensity onto the anode surface becomes less than 50% of the GTA due to the expansion of the arc current channel. Furthermore, it lowers for the higher inner shielding gas flow rate. As a result, the raise in the anode temperature becomes lower and more uniform than the GTA.

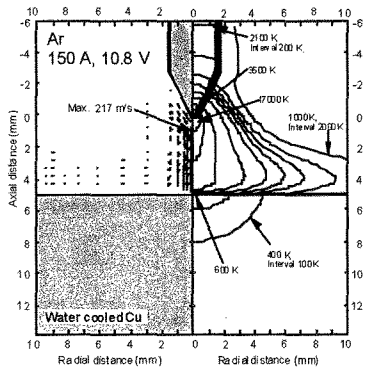

Fig. 3. Two-dimensional distribution of temperature and fluid flow velocity for GTA.

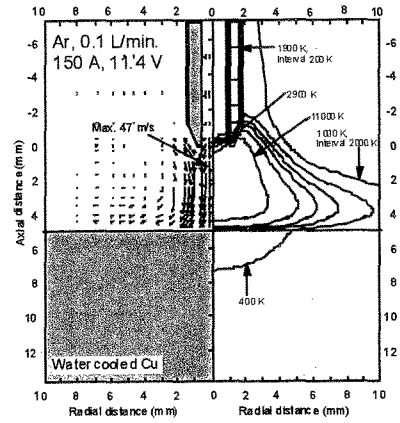

Fig. 4. Two-dimensional distribution of temperature and fluid flow velocity for TCA at inner shielding gas flow rate of 0.1L/min.

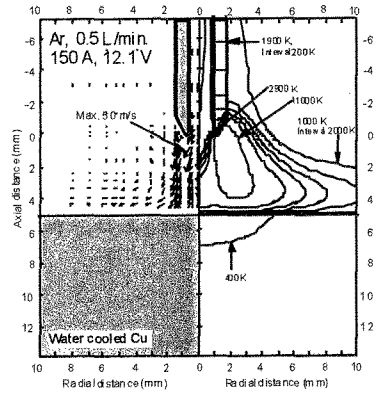

Fig. 5. Two-dimensional distribution of temperature and fluid flow velocity for TCA at inner shielding gas flow rate of 0.5L/min.

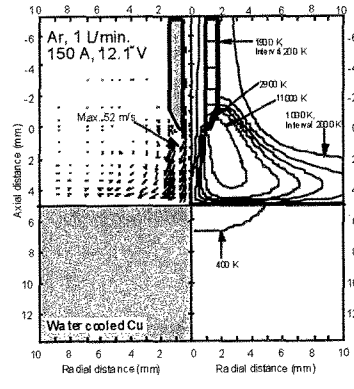

Fig. 6. Two-dimensional distribution of temperature and fluid flow velocity for TCA at inner shielding gas flow rate of 1.0L/min.

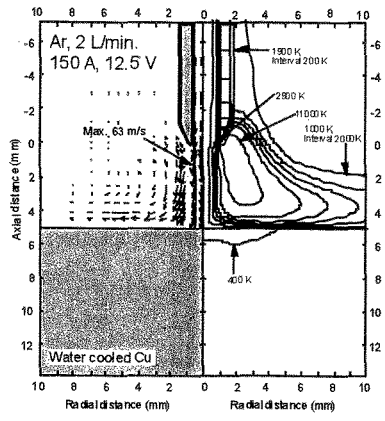

Fig. 7. Two-dimensional distribution of temperature and fluid flow velocity for TCA at inner shielding gas flow rate of 2.0L/min.

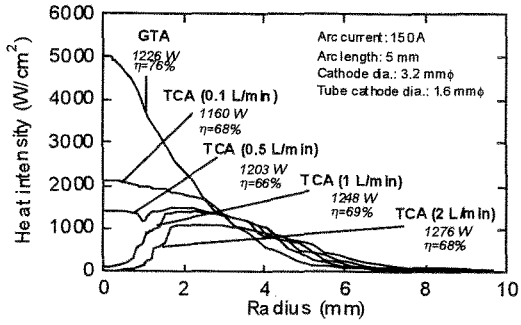

Fig. 8. Radial distributions of heat input intensity on the anode surface.

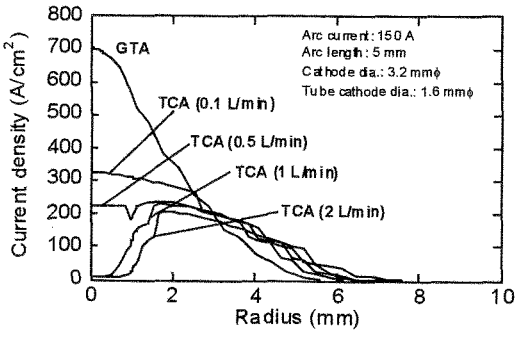

Fig. 9. Radial distributions of current density on the anode surface.

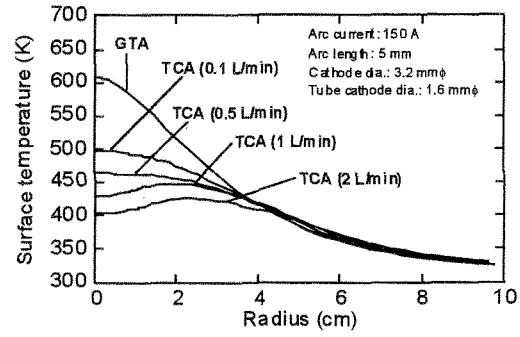

Fig 10. Radial distributions of temperature on the anode surface.

4. CONCLUSIONS

The basic heat source properties of argon TCA at the atmospheric pressure and 150A arc current for various inner shielding gas flow rates were numerically analyzed. Furthermore, the properties were compared with those for the conventional GTA. The main conclusions are summarized as follows:

1) The current density for TCA lowers especially near the cathode than the GTA due to the expansion of the arc current channel caused by the large area of the cathode tip. It leads to the max. plasma temperature of 11000K and the cathode jet velocity of 50m/s which are 60% and 25% of the GTA, respectively.
2) A large volume of uniform high temperature plasma can be produced by controlling the inner shielding gas flow rate. The target material in the arc plasma can be heated uniformly. Moreover, it is heated for long time due to the slow cathode jet.
3) For the anode surface, the max. heat input intensity becomes less than 50% of the GTA because of the lower current density. Furthermore, it lowers also for the higher inner shielding gas flow rate. As a result, the raise in the anode temperature becomes lower and more uniform than the GTA.

References

[1] M. Ushio, et.al., *IEEE Trans. P. S.*, **32**, 108 (2004).
[2] T. Inaba, et.al, *IEEE Trans. D. E. I*, **7**, 684 (2000).
[3] M. Tanaka, et.al., *Vacuum*, **73**, 381 (2004).
[4] Y. Suita, et.al., *Welding Int.*, 8-4 (1994), 269
[5] G.F.Zhang et.at., *Diamond related materials*, **8**, 2148-2151 (1999).
[6] C.-J. Ki and B. Sun, *Thin Solid Films*, **450**, 282 (2004).
[7] M. Tanaka, et.al., *Metal Trans A* **33**, 2043-2052 (2002).
[8] M. Tanaka, et.al., *Plasma Chem. Plasma Process*, **23**, 585-606 (2003).
[9] S. V. Patanker, "Numerical heat transfer and fluid flow" Washington DC, Hemishpere Publishing Corporation, 1980
[10] E. Pfender, "Electric Arcs and Arc Gas heaters, Ch. 6", published in M. H. Hirsh and H. J. Oskam, Gaseous Electronics, Academic Press, NewYork (1978) 291-398.

(Received December 20, 2005; Accepted March 29, 2006)